JOURNAL OF SOLID STATE CHEMISTRY 49, 206–214 (1983)

Vacancy Ordering in $Sc_{1-x}S$

H. F. FRANZEN,[1] R. T. TUENGE,[2] AND L. EYRING

Chemistry Department and the Center for Solid State Science, Arizona State University, Tempe, Arizona 85287

Received January 27, 1983; and in revised form May 6, 1983

This is a study of scandium vacancy ordering in slowly cooled $Sc_{1-x}S$ using high-resolution electron microscopy. Previous X-ray analysis had shown vacancy segregation into alternate (111) planes of the rocksalt substructure. The present study reveals a further incommensurate ordering of the vacancies within the $(111)_c$ planes in approximately every third $(\bar{1}10)_{rhombohedral}$ plane. The incommensurate order was easily destroyed by the irradiation and heating of the electron beam. These observations are discussed in terms of the termination of the wave vector within the Brillouin zone and described in terms of a possible continuous transition to an incommensurate Sc atom population wave.

Introduction

Stoichiometric scandium monosulfide crystallizes in the NaCl-type structure (*1*). The compound, under suitable conditions, exists over a wide range of composition as the result of scandium deficiency (*2*). At about 700°C the vacancies are observed by powder X-ray diffraction to order to form a rhombohedral structure ($R\bar{3}m$) with

$$\begin{pmatrix} a \\ b \\ c \end{pmatrix} = \begin{pmatrix} 1 & \frac{1}{2} & \frac{1}{2} \\ \frac{1}{2} & 1 & \frac{1}{2} \\ \frac{1}{2} & \frac{1}{2} & 1 \end{pmatrix} \begin{pmatrix} a_{\text{cubic}} \\ b_{\text{cubic}} \\ c_{\text{cubic}} \end{pmatrix}$$

in which the vacancies are preferentially located in alternate Sc containing planes along the $[111]_c$ direction (*1, 3*). (Unless otherwise noted the indices shall refer to the cubic substructure.) No evidence of further ordering has previously been reported although the possibilities, either that such ordering accompanies the ordering in alternate planes and has not been observed by X-ray diffraction, or that further ordering occurs within the planes in an independent transition, should be considered. It was in an effort to examine further the defect ordering in $Sc_{1-x}S$ that this work was undertaken.

Experimental Part

Sample Preparation

A defect scandium monosulfide sample was prepared by heating scandium monosulfide at progressively higher temperatures (from about 1300 to 1800°C) in a tungsten Knudsen cell until the congruently vaporizing phase was obtained (*2*). Examination by electron diffraction (see below) of a material prepared in this way with a final radiation quenching of the sample provided no easily interpretable superstructure diffrac-

[1] On leave from the Chemistry Department, Iowa State University and Ames Laboratory, D.O.E., Ames, Iowa 50011, 1981–82.

[2] Present address: Tektronix Inc., Mail Station 50/284, P.O. Box 500, Beaverton, Oregon 97077.

0022-4596/83 $3.00

tion. However, such a sample annealed at 750°C for about 1 day followed by *slow cooling* to room temperature over several days gave evidence of vacancy ordering beyond the $R\bar{3}m$ ordering in the electron diffraction patterns and images.

Electron Microscopy

Specimens from each of the preparations described above were ground in an agate mortar under liquid nitrogen to increase the number of fragments with thin edges suitable for high-resolution transmission electron microscopy (HRTEM). The crystal fragments were suspended in dry acetone and picked up by dipping a microscope grid, covered with a holey carbon film, into the suspension.

The crystal fragments were examined in either a JEM 100B or a JEM 200CX electron microscope equipped with a tilting stage and maintained for high-resolution observations. The techniques employed have been described previously (*4*).

The electron diffraction patterns from the specimens cooled rapidly from > 1300°C gave only diffuse scatter beyond the diffraction from the substructure. No attempt has yet been made to interpret these results.

Results and Comments

Electron diffraction patterns and lattice images of the cubic ⟨111⟩, ⟨100⟩, and ⟨11$\bar{2}$⟩ zones from the specimens annealed at 750°C and cooled slowly are shown in Figs. 1–3. In the ⟨111⟩ and ⟨100⟩ zones the strong diffraction maxima shown in Figs. 1A and 2A correspond to the cubic substructure

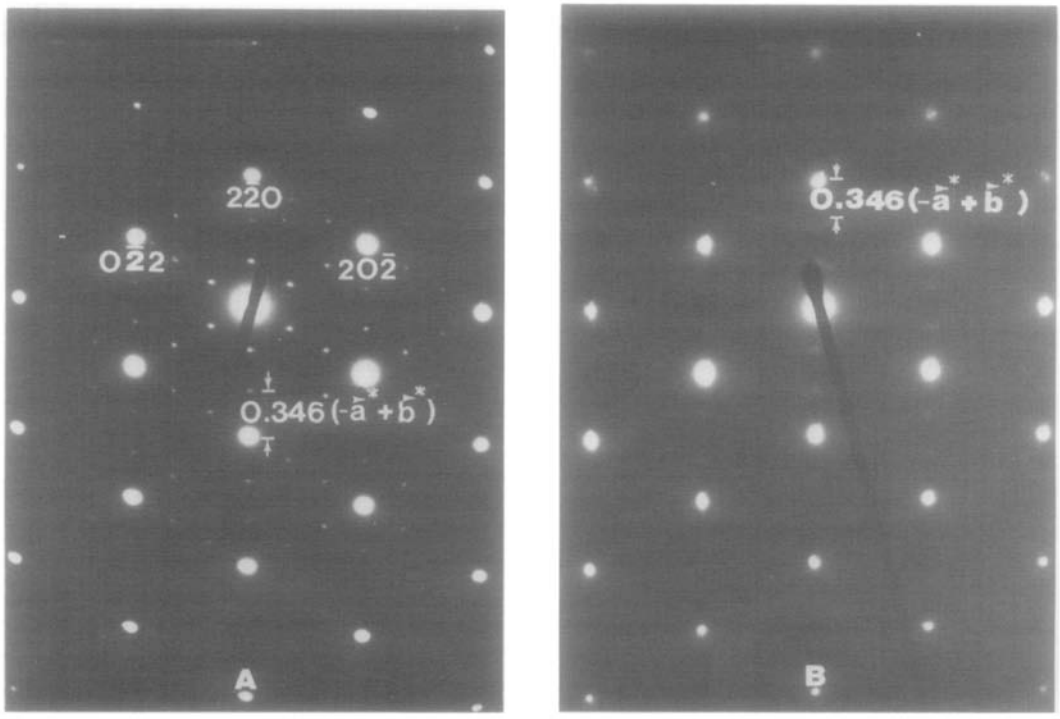

FIG. 1. Electron diffraction patterns from the $\langle 111\rangle_{cubic}$ zone. Notice that the sharp incommensurate superstructure spots in (A) have almost completely disappeared in (B) following electron irradiation. Those remaining are in the vertical direction and are very diffuse.

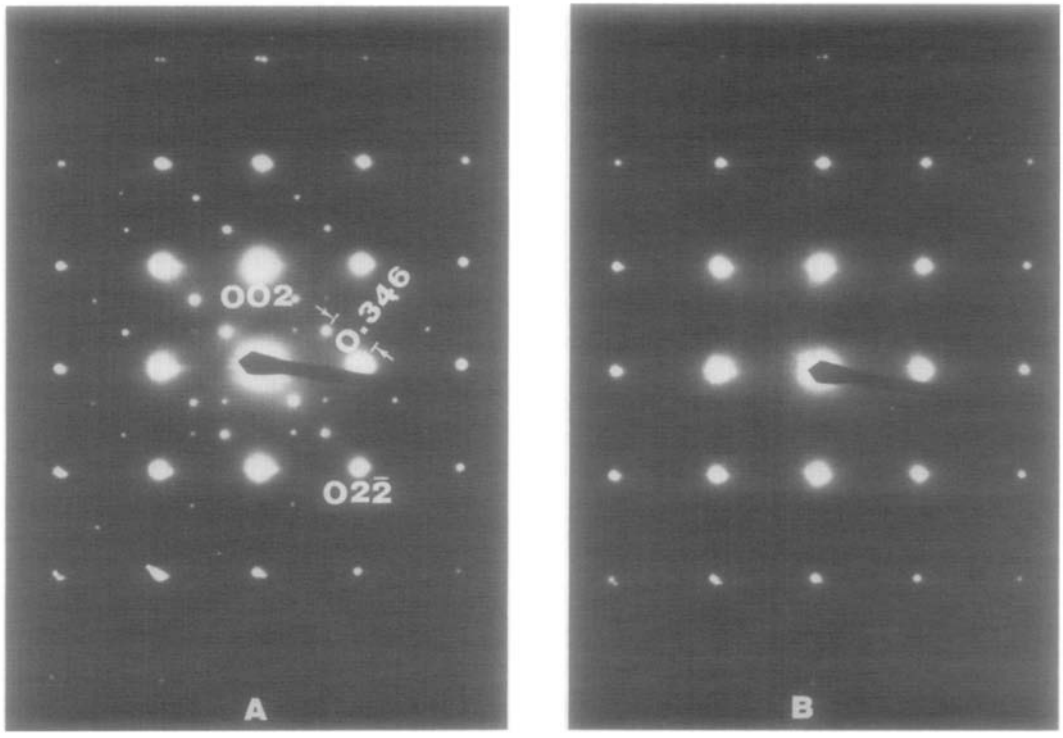

FIG. 2. Electron diffraction patterns from the $\langle 100\rangle_c$ zone. Notice the same incommensurability in (A) as in Fig. 1A and similar fading of these sharp spots as in (B).

and the weaker maxima are superstructure or satellite reflections. The substructure maxima closest to the origin in the $\langle 111\rangle$ zone are the $\langle \bar{1}10\rangle_R$-type reflections of the rhombohedral superstructure and the satellite reflections are located, for example, at $\pm 0.346(-\mathbf{a}^* + \mathbf{b}^*)$ relative to the substructure reflections. The same satellite reflections relative to the same substructure reflections are also observed in the $\langle 100\rangle$ zone.

These incommensurate satellite reflections are also observed in the $\langle 11\bar{2}\rangle$ zone, but in this case these reflections are embedded in an undulating diffuse streak (Fig. 3) containing other maxima as well. The superstructure diffraction maxima will be discussed in terms of vacancy ordering models that are based upon the assumption that the diffraction of the superstructure is incommensurate with the substructure only be-

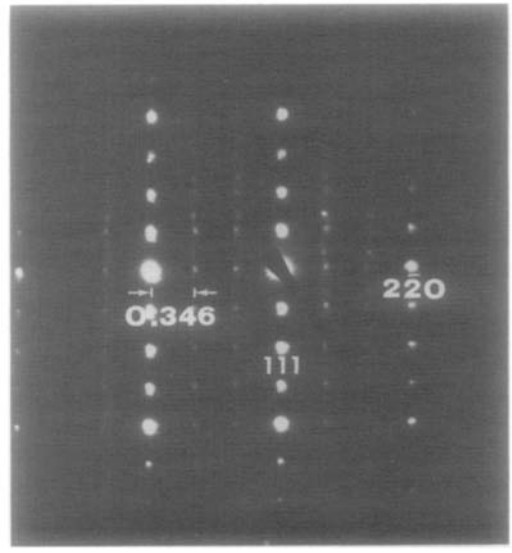

FIG. 3. An electron diffraction pattern from the $\langle 11\bar{2}\rangle_c$ zone. Notice the incommensurate superstructure as before but in this zone undulation of the spots and considerable streaking is apparent.

cause of vacancy ordering. This assumption is based upon the X-ray diffraction evidence that the lattice is negligibly distorted upon symmetry lowering via vacancy ordering.

It was observed that the satellite maxima in the ⟨111⟩ zone are very sensitive to annealing by the electron beam. After exposure to the beam, which may have raised the temperature of the sample as high as 300°C, the satellite reflections in two of the three directions were eliminated and the remaining maxima in the $\pm 0.346(-\mathbf{a}^* + \mathbf{b}^*)$ positions were weak and diffuse (Fig. 1B). This observation indicates that the ordering under discussion here occurs independently of, and at a considerably lower temperature than, the $R\bar{3}m$ ordering. The observation also suggests that the ordering in individual domains corresponds to a single **k** vector, e.g., $0.346(-\mathbf{a}^* + \mathbf{b}^*)$, and that the occurrence of satellites in directions corresponding to other **k** vectors in the star, as observed in the ⟨111⟩ zone, is the result of superposition of diffraction from three types of domains corresponding to ordering in the three independent directions. This suggestion is also supported by the observation in the ⟨100⟩ zone that the satellite reflections in the two different directions have two different sets of intensities indicating that the electron beam samples two types of domains with one type predominating. Accordingly, the interpretation given below is in terms of ordering (called tertiary here) corresponding to the single **k** vector $0.346(-\mathbf{a}^* + \mathbf{b}^*)$, i.e., in terms of ordering among $(\bar{1}10)_R$ planes. The superstructure reflections in the ⟨100⟩ zone also become diffuse upon irradiation (Fig. 2B).

Figure 4A depicts a $\langle 11\bar{2}\rangle$ lattice image of a thin crystal taken in the JEM 100B micro-

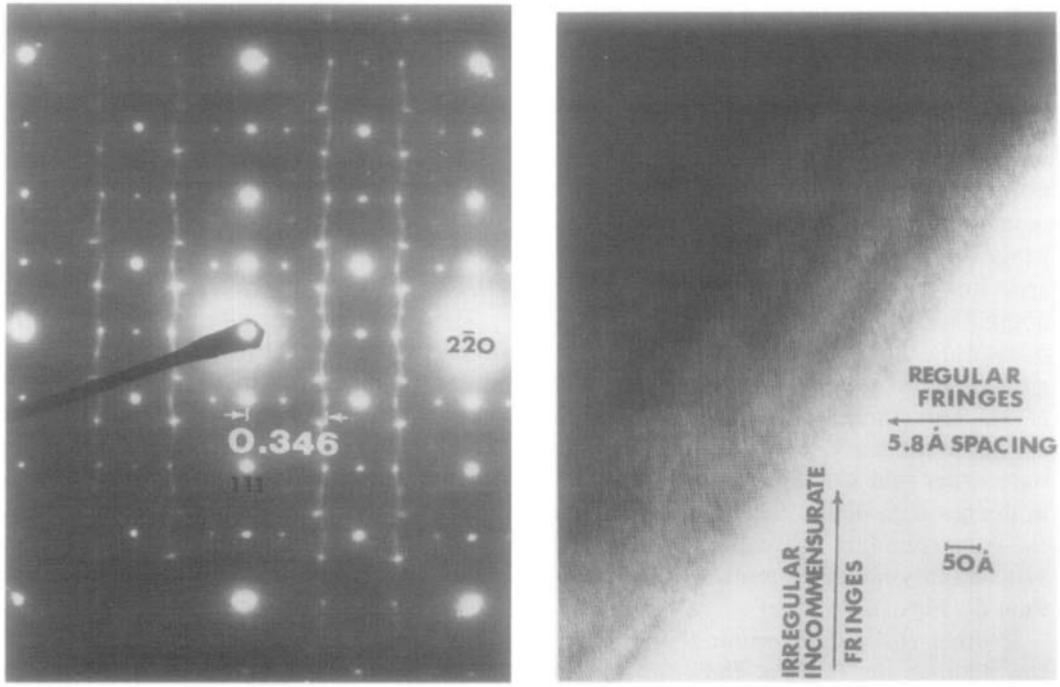

FIG. 4. A $[11\bar{2}]$ zone diffraction pattern and image of a thin crystal with irregular tertiary order. Notice the incommensurate streaking with the embedded diffraction maxima that correspond to the irregular vertical fringes of the image.

scope. The alternating occupancy of the (111) planes indicated by doubling the unit cell along ⟨111⟩ is apparent in the regularly spaced horizontal rows of image spots having about 5.8 Å spacing. In contrast, the rows of spots in the image which are more or less vertical clearly give rise to the wavy rows of vertical spots with diffuse streaks between in the diffraction pattern (Fig. 4B). There are preferred orientations in the rows of image spots, some are vertical, others are canted about 16° either to the right or to the left, and they have varied spacing. The corresponding disordered orientations in the crystal give rise in the diffraction pattern (Fig. 4B) to the three incommensurate spots joined by diffuse streaks to either side of the principal diffraction maxima. The three spots are streaked such that the central one along $[2\bar{2}0]$ is elongated perpendicular to that direction while those at about 16° to either side are elongated along the radius toward the associated reflection. Every strong spot, including those arising from a doubling of $d_{2\bar{2}0}$ is so decorated. This doubling, which suggests further ordering of vacancies in every second $(\bar{1}10)_R$ plane, would give fringes of 3.6 Å spacing that are not observed and are probably below the resolution in this image. Uneven vertical fringes of about 10.8 Å are apparent corresponding to the incommensurate spots of about $\frac{1}{6}$ $(2\bar{2}0)$. There appears to be no commensurate diffraction occurring in the region between the substructure rows along [111]. This image (Fig. 4A) catches the crystal in the early stages of the loss of tertiary order that was even further advanced in images obtained in the JEM 200CX, and the corresponding diffraction pattern (Fig. 4B) similarly indicates more superstructure than do Figs. 1–3.

In other zones that contain the ⟨110⟩ vector, such as the ⟨111⟩ or the ⟨100⟩ already mentioned, the incommensurability becomes streaked perpendicular to the $[2\bar{2}0]$. In that case the final diffuse scatter is along only one of the three possible directions. In Fig. 5, however, this phenomenon, including the transverse streaking, is observed to occur strongly in all three directions. There is a distinct loss of hexagonal symmetry in this case, due to irregular streaking. In the ⟨100⟩ zone, as seen in Fig. 2B, the diffuse scatter after irradiation suggests a similar behavior but at a much later stage of disorder.

The JOEL 200CX microscope was used to obtain through-focus high-resolution images of a crystal fragment. The image of the thin edge was averaged, Fig. 6 (*5*), and compared to that calculated on the basis of the vacancy model discussed below and illustrated in Fig. 7. The images, observed and calculated, are from the $[3\bar{1}0]_m$ zone of the pseudo-orthorhombic structure. The match, which is quite satisfactory, is shown in Fig. 6. The statistical comparisons, fractional mean absolute difference, FMAD, and the correlation coefficient, CC, would be 0 and 1, respectively, for a perfect match. The numbers obtained are as good as those of the best matches found when the structures are known. The microscope and specimen conditions are given in the legend of Fig. 6.

Discussion

The diffraction results pertaining to ordering within the $(\bar{1}10)_R$ planes (Figs. 1 and 2) can be discussed in two stages, first as though the superstructure exactly tripled the periodicity, i.e., as though the ordering corresponded to $\frac{1}{3}(-\mathbf{a}^* + \mathbf{b}^*)$, second to account for the fact that the scalar coefficient is not $\frac{1}{3}$, but 0.346, i.e., for the incommensurate nature of the ordering.

A vacancy ordering model that yields a structure consistent with the hypothetical **k** vector $\frac{1}{3}(-\mathbf{a}^* + \mathbf{b}^*)$ places the vacancies, which are located in alternate planes along the [111] cubic direction, in every third $(\bar{1}10)_R$ rhombohedral plane. A pseudo-

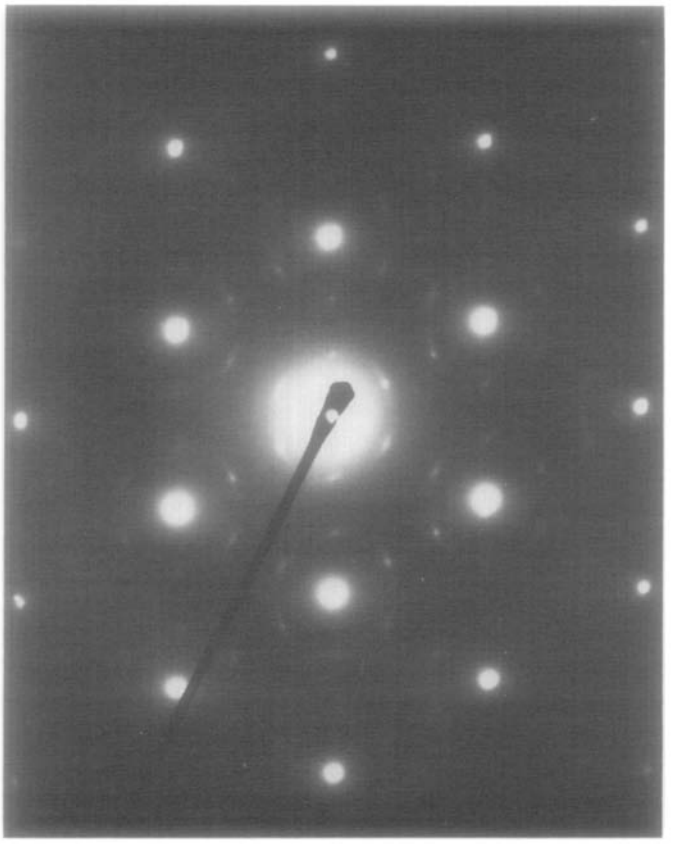

FIG. 5. An electron diffraction pattern of a crystal taken along ⟨111⟩ showing the incommensurate superstructure and transverse streaking that occurs as tertiary order is being lost.

orthorhombic cell with

$$\begin{pmatrix} a \\ b \\ c \end{pmatrix} = \begin{pmatrix} \frac{1}{2} & \frac{1}{2} & -1 \\ -\frac{3}{2} & \frac{3}{2} & 0 \\ 2 & 2 & 2 \end{pmatrix} \begin{pmatrix} a_{\text{cubic}} \\ b_{\text{cubic}} \\ c_{\text{cubic}} \end{pmatrix}$$

and space-group symmetry $C2$ (Fig. 7) results. The scandium positions have three different occupancies, the positions at $z = 0, \frac{1}{3}$, and $\frac{2}{3}$ contain the vacancies, with the positions in these layers related to 0,0,0 and $\frac{1}{3},0,\frac{2}{3}$ having one fractional occupancy (ϕ_1) and those related to $\frac{1}{2},\frac{1}{6},0$; $0,\frac{1}{3},0$; $\frac{1}{3},\frac{1}{3},\frac{2}{3}$; and $\frac{1}{6},\frac{1}{6},\frac{1}{3}$ having another (ϕ_2). The positions in the layers at $z = \frac{1}{6},\frac{1}{2}$, and $\frac{5}{6}$ (i.e., those related to $\frac{1}{3},0,\frac{1}{6}$; $\frac{1}{3},\frac{1}{3},\frac{1}{6}$; $0,0,\frac{1}{2}$; $\frac{1}{2},\frac{1}{6},\frac{1}{2}$; $0,\frac{1}{3},\frac{1}{2}$; and $\frac{1}{6},\frac{1}{6},\frac{5}{6}$) are completely occupied. The ideal tertiary structure can be described as having the vacancies concentrated in alternate planes along the c axis and tending to concentrate within these planes in every third plane along the unique b axis of the monoclinic cell.

Since the **k** vector $\frac{1}{3}(-\mathbf{a}^* + \mathbf{b}^*)$ does not terminate at a special symmetry point of the Brillouin zone, the fact that the vacancy ordering is incommensurate is not surprising from the point of view of Landau theory (*6*). As has been pointed out by Haas (*7*), phase transitions to stable incommensurate structures are expected under these circumstances. However, the real space

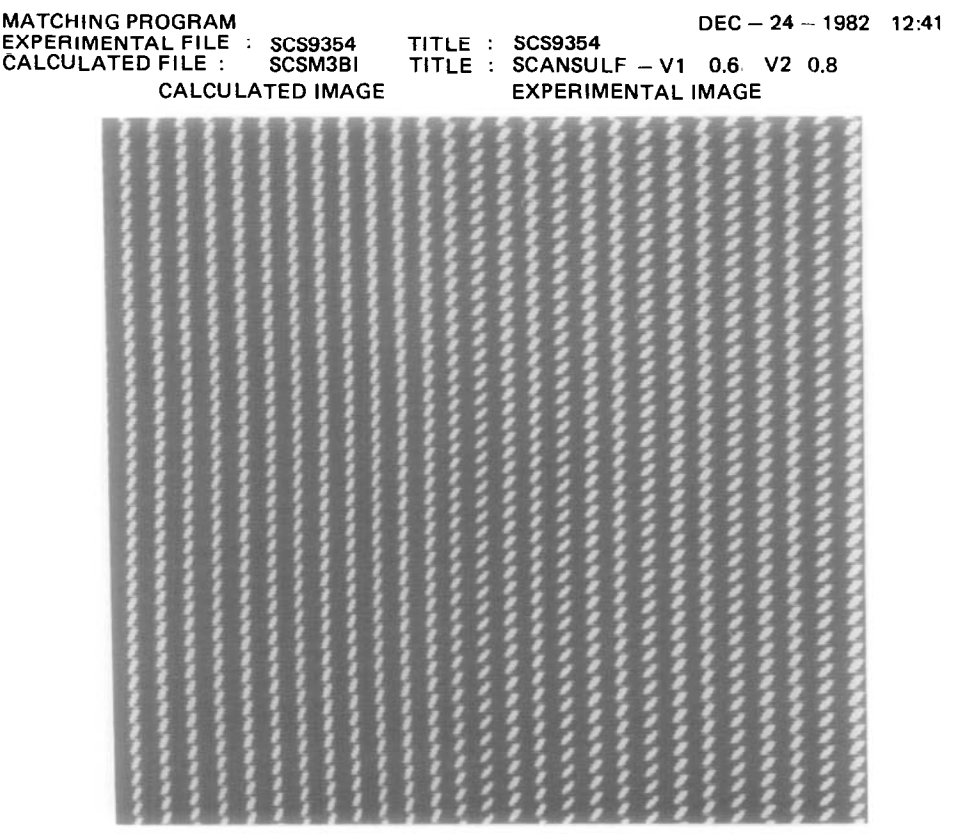

FIG. 6. A comparison of the averaged thin crystal image with that calculated on the basis of the vacancy ordering model proposed for the pseudo-orthorhombic unit cell of Fig. 7. The calculation was made for the following conditions of the microscope and specimen: C_s = 1.2 mm, depth of focus 200 Å, beam divergence 0.002 rad, aperture radius 1 Å^{-1}, defocus −700 Å, specimen thickness 45 Å. Imaged down the $[3\bar{1}0]_m$ zone.

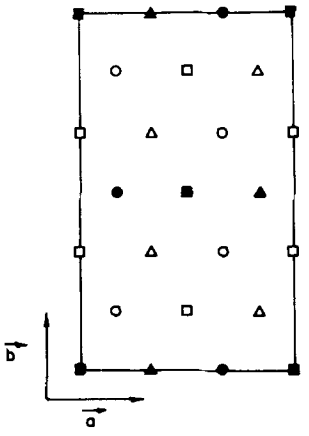

mechanism whereby the vacancies can order in an incommensurate fashion is not immediately obvious.

Following Fujiwara (*8*) it is proposed that corresponding to the given **k** vector there is a periodic fractional occupancy function, $\phi(x)$, with period different from an integral

FIG. 7. The unit cell of the structure that results from vacancy ordering in every third $(\bar{1}10)$ rhombohedral plane. The metal atom positions are at heights z = 0,$\frac{1}{2}$ (□), z = $\frac{1}{8}$,$\frac{5}{8}$ (△), and z = $\frac{3}{8}$,$\frac{7}{8}$ (○). The blackened markers denote the vertical planes in which the vacancies are concentrated in the ideal structure.

multiple of the lattice spacings (Fig. 8). This function yields two values of the fractional occupancy, ϕ_1 and ϕ_2, as a function of the distance along the perpendicular to the planes, and because of the difference in period is an incommensurate population wave.

Letting L be the period of the population wave, and for the purpose of illustration taking the population wave to be a square wave,

$$\phi = \phi_1 \qquad \text{when } 0 \le x \le L/6$$

$$\phi = \phi_2 \qquad \text{when } L/6 < x \le L/2$$

and $\phi(x)$ can be expanded in a Fourier series:

$$\phi(x) = \frac{\phi_1 + 2\phi_2}{3} + \sum_{m=0}^{\infty} \frac{2(\phi_1 - \phi_2)}{m\pi} L \sin\frac{m\pi}{3} \cos 2m\pi\frac{x}{L}.$$

Letting n label the planes, the contribution of the population wave to diffraction by the $(\bar{h}h0)_R$ planes is given by (*6*);

$$FF^* = \left| \sum_{n=1}^{N-1} \phi(n) f_{Sc} \exp 2\pi i n h \right|^2$$

or

$$FF^* = \left| \sum_{n=1}^{N-1} \frac{\phi_1 + 2\phi_2}{3} f_{Sc} \exp 2\pi i n h + \sum_{m=0}^{\infty} \frac{2\phi_1 - \phi_2}{m\pi} L f_{Sc} \sin\frac{m\pi}{3} \sum_{n=1}^{N-1} \left(\exp 2\pi i n\left(l + \frac{m}{L}\right) + \exp 2\pi i n\left(l - \frac{m}{L}\right)\right)\right|^2$$

The first term can make a significant contribution only if h is an integer, i.e., this term contributes only to the substructure reflections. The second term can contribute significantly only if $h \pm m/L$ (m = integer) is an integer. The observed satellite reflections follow from $L = 2.89$ and $m = 1$. The $m = 2$ and higher order satellite reflections are not generally observed presumably because the actual population wave is not a square wave and higher harmonics do not enter significantly into the Fourier Expansion.

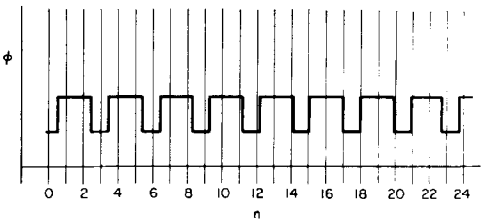

FIG. 8. Illustration of the real space result of the incommensurate **k** vector. The fraction occupancy function (ϕ) is plotted vs distance (square wave) where the integral distances correspond to consecutive $(\bar{1}10)_R$ planes (perpendicular to the wave direction).

The incommensurate population wave terms (those that vanish with $\phi_1 = \phi_2$) do not contribute to the substructure reflections since these contributions would occur with m an integral multiple of 3 and such terms vanish because of the factor $\sin m\pi/3$.

Thus a model of vacancy ordering in $Sc_{1-x}S$ that is consistent with the sharp diffraction maxima is

$$Fm3m \xrightarrow{700°C} R\bar{3}m \xrightarrow{\sim 300°C} C2,$$

where the last exhibits incommensurate diffraction maxima because the vacancies are not exactly in every third rhombohedral $(\bar{1}10)_R$ plane but occasionally occur in the second $(\bar{1}10)_R$ plane, as shown in Fig. 8. According to Landau theory (*6*) both of these order–disorder transitions can occur continuously. The reciprocal spacing $0.346(-\mathbf{a}^* + \mathbf{b}^*)$ implies that on an average 1 vacancy plane in 13 occurs on every second $(\bar{1}10)_R$ plane. Although it is not a regular ordering, this should be reflected in a variation in the spacing in the images. The incommensurate fringes in Fig. 4 show this. The streaking and additional spots in the $\langle 11\bar{2}\rangle$ zone indicate further modulations of the population wave in the [111] direction. Since the diffuse streaking has a wavy char-

acter it appears likely that this modulation is alternative to, rather than coexistent with, the incommensurability discussed above, and that the streaks and spots coexisting on the pattern result from a variety of domains with a variety of incommensurate vacancy orderings. However, the definitive interpretation of these diffraction results hinges upon additional information, perhaps from precise X-ray diffraction.

Acknowledgments

Helpful discussion with J. M. Cowley and A. Rae Smith as well as support from NSF Research Grant DMR 8108306 and NSF Microscope Facility Grant CHE 7916098 (The Regional Instrumentation Center for High Resolution Electron Microscopy) are gratefully acknowledged.

References

1. J. P. DISMUKES AND J. G. WHITE, *Inorg. Chem.* **3,** 1220 (1964).
2. H. F. FRANZEN AND R. T. TUENGE, *J. Chem. Phys.* **65,** 2400 (1976).
3. H. F. FRANZEN AND J. A. MERRICK, *J. Solid State Chem.* **33,** 371 (1980).
4. S. IIJIMA, *Acta Crystallogr. Sect. A* **29,** 18 (1973).
5. A. RAE SMITH AND L. EYRING, *Ultramicroscopy* **8,** 65 (1982).
6. L. LANDAU AND E. LIFSHITZ, "Statistical Physics," pp. 430–456, Pergamon, Elmsford, N.Y. (1959).
7. C. HAAS, *Phys. Rev.* **140,** A863 (1965).
8. K. FUJIWARA, *J. Phys. Soc. Jpn.* **12,** 7 (1957).